Swiss J Geosci (2015) 108:345–359
DOI 10.1007/s00015-015-0201-4

Sequence stratigraphy and depositional environments of Late Cretaceous–Early Palaeogene succession, North Eastern Desert, Egypt

Mohamed Youssef[1,2] · **Mahmoud Hefny**[1]

Received: 25 March 2015 / Accepted: 21 September 2015 / Published online: 14 November 2015

Abstract The foraminiferal contents and geochemistry of 199 samples collected from three surface sections in the southern Galala Sub-basin, North Eastern Desert of Egypt, have been studied in detail. From south to north these sections are situated at Gebel Tarboul, Wadi Tarfa, and Bir Dakhl. The results allow reconstructing of the depositional environments and high resolution sequence stratigraphy of the Upper Cretaceous–Palaeogene succession. The quantitative and qualitative distribution patterns of benthic foraminifera of the Upper Cretaceous–Lower Palaeogene succession suggests a depositional environment from outer neritic to bathyal, at 200 to ~700 m water-depth. Based on sequence stratigraphic analyses, ten complete third order depositional sequences have been recognized. These depositional sequences from base to top are as follows: CaSGB-1 sequence, CaSGB-2 sequence, MaSGB-1 sequence, MaSGB-2 sequence, DaSGB sequence, Da/SeSGB sequence, SeSGB sequence, ThSGB sequence, Sp/YpSGB, and YpSGB sequence. These sequences are controlled by both eustatic sea-level changes and tectonic movements that prevailed during deposition.

Keywords Depositional environments · High resolution sequence stratigraphy · Cretaceous · Palaeogene · Eastern Desert · Egypt

Handling editor: W. Winkler.

Electronic supplementary material The online version of this article (doi:10.1007/s00015-015-0201-4) contains supplementary material, which is available to authorized users.

✉ Mohamed Youssef
mymohamed@ksu.edu.sa; myousefgeology@gmail.com

Mahmoud Hefny
mahmoud.hefny@svu.edu.eg

[1] Department of Geology, Faculty of Science, South Valley University, 83523 Qena, Egypt

[2] Department of Geology and Geophysics, College of Science, King Saud University, P. O. Box. 2455, Riyadh 11451, Saudi Arabia

1 Introduction

The Cretaceous–Palaeogene interval provides one of the best opportunities to calibrate depositional sequences against an integrated stratigraphic framework. This can be examined in the rocks of Cretaceous–Palaeogene age that are widely distributed in Northern Africa along the southern margin of the Tethys Ocean. On the Egyptian territory, the Cretaceous–Palaeogene exposures are well-known in many localities ranging from Sinai, Eastern Desert, to the Western Desert. The stratigraphy and sedimentology of the outcropping Upper Cretaceous–Lower Palaeogene succession in the Eastern Desert of Egypt have been studied by several authors since (e.g. Awad and Abdallah 1966). The interpretations of the synsedimentary tectonics of the Upper Cretaceous–Paleocene carbonate-dominated strata in the Galala area (Kuss 1992; Moustafa and Khalil 1995) form the basis for further detailed investigations (Scheibner et al. 2000, 2001). In the studied Southern Galala Sub-basin, in the northern part of Egyptian territory, where the unstable shelf is located, marine sedimentary sections across the Cretaceous/Palaeogene (K/Pg) interval are widely distributed and preserved in the Sudr, Dakhla, Tarawan and Esna formations. Intensive work on the stratigraphy, biostratigraphy and sedimentology of the outcropping Cretaceous–Palaeogene succession in the Eastern Desert of Egypt had been done (Abdel-Kireem and

Abdou 1979; Bandel and Kuss 1987; Bandel et al. 1987; Hendriks et al. 1987; Kuss and Leppig 1989; Kuss et al. 2000, Ismail et al. 2009; Scheibner and Speijer 2009; Höntzsch 2011; Ismail 2012; and Hefny and Youssef 2015). The present study is an attempt to contribute to finding evidence in support of sequence stratigraphical interpretations. The present study is aimed at: (1) constructing of the depositional environments for the study area; and (2) elucidating the sequence stratigraphic architecture that was developed during the pulsatory third-order relative sea-level cycles through using the available data.

2 Geological setting

During the early Late Cretaceous, Egypt was situated at the southern margin of the Neotethys at ca. 5° northern palaeolatitude (Philip and Floquet 2000). The Cretaceous–Palaeogene rocks are well exposed in the northern part of the Eastern Desert. However, outcrops of lower Upper Cretaceous (Cenomanian-Turonian) strata are comparatively rare and little is known in detail about their facies and depositional environment. The Campanian–Eocene systems produced widespread sediments in Eastern Desert, which were formed during a major transgressive period when the sea extended up to some 1000 km inland of the present coast (Picard 1943; Said 1962; Garfunkel and Bartov 1977).

The investigated area (Fig. 1) represents a segment of the northern passive margin of the Afro-Arabian plate during the Late Triassic–Jurassic opening of the Neotethys. The extensional tectonic processes resulted in the formation of east–west striking northward-deepening half-grabens that were mostly covered by the Late Triassic–Early Cretaceous seas, depending on sea level fluctuations (Scheibner et al. 2001). Beginning with the initial stages of the collision between Africa and Eurasia during the Turonian stage, a dextral transpressive reactivation of the half-grabens took place along the North African-Arabian plate boundary (e.g. Aal and Lelek 1994; Moustafa and Khalil 1995). Consequently, a system of inverted, uplifted and folded grabens was formed, and was called the Syrian Arc System and 'unstable shelf' (Krenkel 1925; Said 1962). The structures here were mainly active during the Late Santonian (Kuss et al. 2000; Rosenthal et al. 2000). But there is evidence of several Early Eocene tectonic pulses on the same structures in the Galala Mountains that have been recently discussed in details by Höntzsch et al. (2011). The Galala Mountains in the Eastern Desert, together with areas on western Sinai, represent a southern branch of the Syrian Arc and it is called the Northern Galala/Wadi Araba High (Kuss et al. 2000), and is characterized by Late Cretaceous uplift in the north and subsidence further to the south.

Fig. 1 Satellite image of the Southern Galala Sub-basin, Eastern Desert, Egypt. Shown are the affecting structures, distribution of the formations, and the location of studied sections, which run in transect A-B parallel to the Gulf of Suez. The strike directions of the Wadi Araba and North Esh El-Mallaha faults (related to Mesozoic–Palaeogene tectonics) and the Gulf of Suez faults (related to the Miocene opening of the Gulf) lie perpendicular to each other ▶

3 Lithostratigraphy

The base of the studied interval is characterized by Upper Cretaceous massive white and creamy chalk and chalky limestone beds with intercalations of light gray calcareous shale and argillaceous limestone (Sudr Formation, Figs. 2, 3, 4). This formation unconformably underlies a sequence of cherty limestone of the Thebes Group at Gabel Tarboul (Fig. 4), northern Esh El Mallaha area, a sequence of gypsiferous shale of the Dakhla Formation in Wadi Tarfa (Fig. 2b), and a sequence of brownish yellow marly shale of the Upper Paleocene Esna Formation in the Bir Dakhl section (Fig. 3a; Hefny and Youssef 2015). The Upper Cretaceous–Palaeocene Dakhala Formation represents yellowish to greyish fissile shales with argillaceous limestone and clay interbeds. It is sandwiched between the Sudr Formation below and Tarawan Formation above in Wadi Tarfa. In the Gabel Tarboul and Bir Dakhl sections, the Palaeocene Dakhla passes laterally into the Sudr Formation. The Tarawan Formation includes the Upper Paleocene thick bed of chalk and chalky limestone, which in the study area was deposited as outer shelf- basinal chalks/limestones protected from shallow water influences. The Esna Formation (Fig. 2a) comprises Upper Paleocene to Lower Eocene laminated, green, grey-green, brownish or blackish-grey shale, sandy shale and marl, either fissile or massive, and some gypsum veinlets shale, with more calcareous components toward the top. The Esna Formation was deposited as basinal marls without shallow water input.

4 Materials and methods

In the present study, 199 samples were collected from three surface sections in the Northern Galala/Wadi Araba High. The three sections from south to north are as follows: Gebel Tarboul (Eash El-Mellaha range) (EM): N27°50′38″, E33°09′59″, Wadi Tarfa section (WT): N28°13′7.5″, E32°13′°49″, Bir Dakhl section (BD): N28°40′57″, E32°34′08″. In the Gebel Tarboul section (Fig. 4), the studied interval includes the Sudr Formation, which is divided into two members: The Markha Chalk Member (Campanian) and the Abu Zeneima Member (Maastrichtian). This formation unconformably underlies a sequence of cherty limestone of the Thebes Group. The

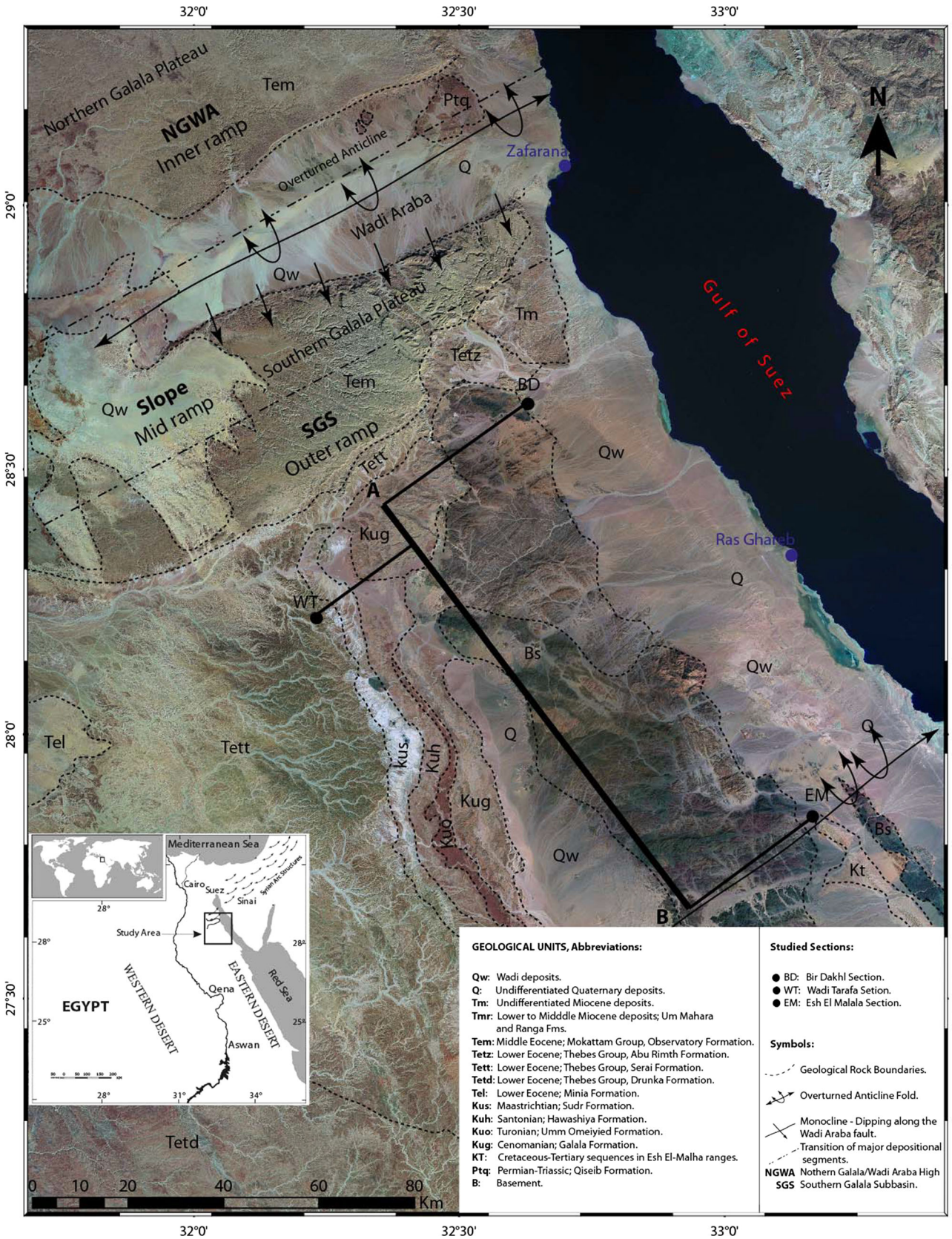
32°0'
32°30'
33°0'
29°0'
28°30'
28°0'
27°30'
Northern Galala Plateau
NGWA
Inner ramp
Tem
Ptq
Overturned Anticline
Zafarana
Q
Wadi Araba
Qw
Gulf of Suez
N
Southern Galala Plateau
Tm
Tetz
Qw Slope
Mid ramp
Tem
BD
SGS
Outer ramp
Tett
Qw
A
Kug
Ras Ghareb
Q
WT
Bs
Qw
Tel
Tett
kus
Kuh
Q
Q
Kug
Kuo
EM
Bs
Qw
Kt
B
Tetd
Mediterranean Sea
Cairo
Suez
Sinai
Syrian Arc Structures
Study Area
EGYPT
WESTERN DESERT
EASTERN DESERT
Red Sea
Qena
Aswan
0 10 20 40 60 80 Km
GEOLOGICAL UNITS, Abbreviations:
Qw: Wadi deposits.
Q: Undifferentiated Quaternary deposits.
Tm: Undifferentiated Miocene deposits.
Tmr: Lower to Midddle Miocene deposits; Um Mahara and Ranga Fms.
Tem: Middle Eocene; Mokattam Group, Observatory Formation.
Tetz: Lower Eocene; Thebes Group, Abu Rimth Formation.
Tett: Lower Eocene; Thebes Group, Serai Formation.
Tetd: Lower Eocene; Thebes Group, Drunka Formation.
Tel: Lower Eocene; Minia Formation.
Kus: Maastrichtian; Sudr Formation.
Kuh: Santonian; Hawashiya Formation.
Kuo: Turonian; Umm Omeiyied Formation.
Kug: Cenomanian; Galala Formation.
KT: Cretaceous-Tertiary sequences in Esh El-Malha ranges.
Ptq: Permian-Triassic; Qiseib Formation.
B: Basement.
Studied Sections:
BD: Bir Dakhl Section.
WT: Wadi Tarafa Setion.
EM: Esh El Malala Section.
Symbols:
Geological Rock Boundaries.
Overturned Anticline Fold.
Monocline - Dipping along the Wadi Araba fault.
Transition of major depositional segments.
NGWA Nothern Galala/Wadi Araba High
SGS Southern Galala Subbasin.

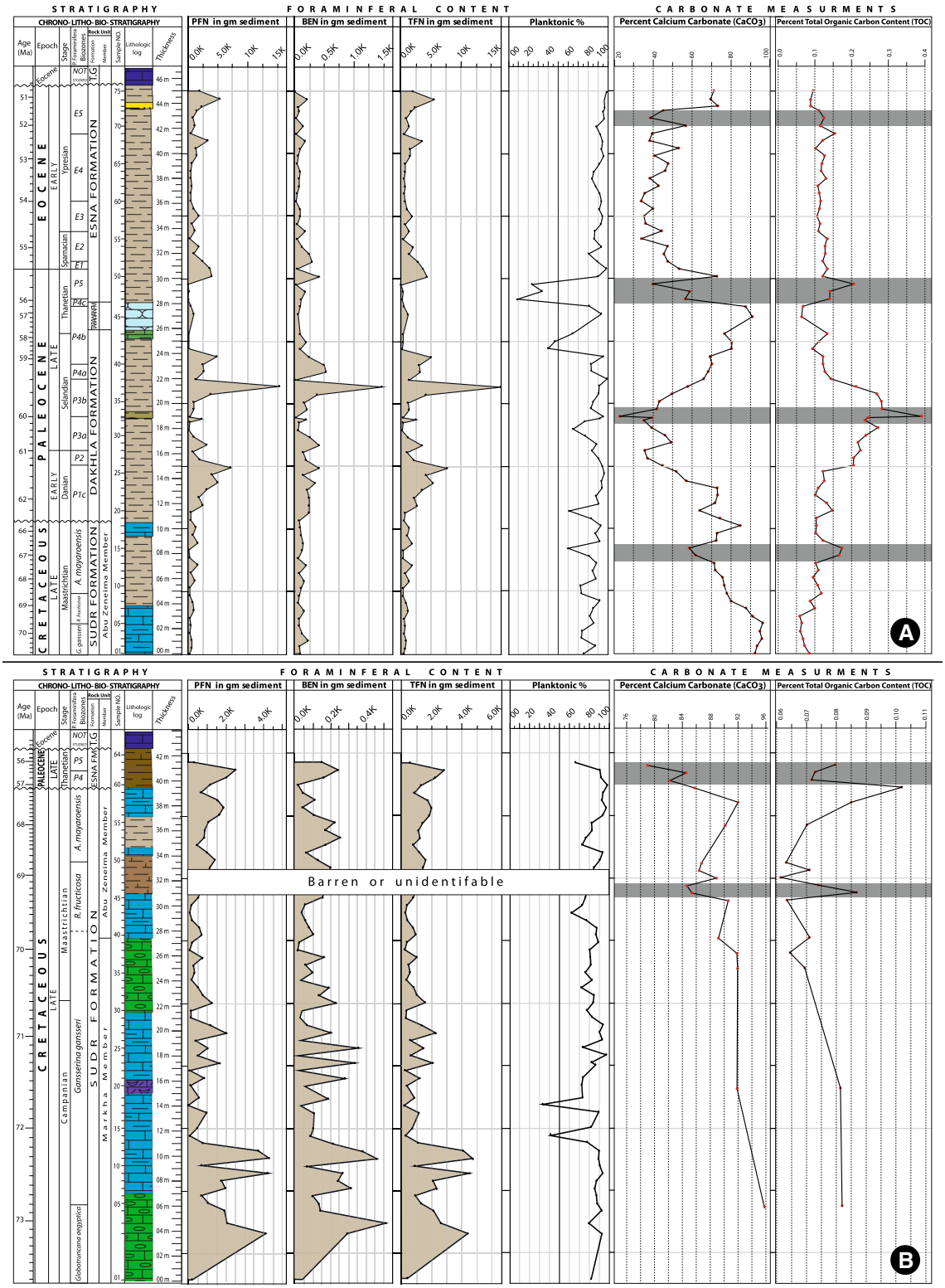

Fig. 2 **a** Wadi Tarfa section and (**b**) Bir Dakhl section. Planktonic foraminiferal number (PFN), benthic foraminiferal number (BFN), total foraminiferal number (TFN), and planktonic percent (P%) recorded in North Eastern Desert versus planktonic biozonation (Berggren et al. 1995). Organic carbon content together with total CaCO3 content in percent are plotted vs. integrated stratigraphy in Wadi Tarfa and Bir-Dakhl sections. *Grey shaded bars* indicate intervals of very low values in carbonate content

exposed interval in Wadi Tarfa section comprises the Sudr, Dakhala, Tarawan, Esna, and Thebes formations. In the Bir Dakhl section the Sudr and Esna formations are exposed.

In sequence stratigraphic studies, microfossils are used to correlate local depositional cycles into a regional framework (e.g. Haq et al. 1987). Among the most used and readily studied microfossils are the foraminifera. We quantified the foraminiferal planktonic percent number (P%) and carried out a benthic foraminiferal morphogroup analyses. Based on morphology, life position, feeding habitat and environment, four benthic foraminiferal assemblages (biofacies A–biofacies D) have been recognized (Table 1). Total carbon (TC) and total organic carbon (TOC) were determined (Bengtsson and Enell 1986).

5 Results

5.1 Organic geochemistry

The organic geochemistry was carried out on 92 samples derived from the Wadi Tarafa and Bir Dakhl sections. The results are displayed as black lines on a 10 based logarithmic scale in Fig. 2. In general and in particular the Wadi Tarafa sediments are characterized by low total organic carbon contents. A strong control by prevailing high sedimentation rates, hyperthermal events and siliciclastic dilution on the platform can be inferred.

5.1.1 Calcium carbonate content ($CaCO_3$)

It is clearly visible at Wadi Tarfa (Fig. 2a) that the calcium carbonate content of the studied rocks varies inversely with TOC throughout the section. The lowermost argillaceous limestone of the Sudr Formation records the highest $CaCO_3$ values fluctuating from 88 to 96 % (average = 92 %), while the upper marly shale shows a distinct decline in $CaCO_3$ content ranging from 80 % to 58 % (average = 69 %). The uppermost part at 10.2 m shows 85 % $CaCO_3$ which is again characterized by marlstone/limestone. The carbonate content of the Dakhla Formation steadily declines from 63 to 35 % (average = 49 %), with an exceptional depletion to less than 22 % at 19.2 m. This is followed by a gradual increase in values from 40 to 80 % (average = 60 %). The chalk of the Tarawan Formation records high values of 91 % carbonate content at 27.3 m. The hemipelagic Esna Shale shows more or less constant low values between 33 and 58 % (average = 45.5 %), followed by 70 and 73 % carbonate content in the uppermost part of the studied section (from 44.1 to 45 m). Generally, the Bir Dakhl section (Fig. 2b) is rich in calcium carbonate (more than 86 %) because of prevalent marlstone/limestone and limestone facies. It shows two CaCO3 minima; one in the upper part of the Sudr Formation (84 % at 32.1 m), and the other in the upper part of Esna Shale Formation (79 % at 41.7 m).

5.1.2 Total organic carbon (TOC)

The amount of the organic matter in the analyzed samples is variable according to the type of lithology and their characteristic attributes. Generally, in Wadi Tarfa, the TOC values are characterized by fluctuations at low levels from 0.06 to 0.4 % (Fig. 2a). A TOC maximum is reached at 20.6 m with 0.39 %. The lowermost argillaceous limestone of the Sudr Formation records the lowest TOC values fluctuating from 0.06 to 0.1 %. The uppermost marly shale shows values from 0.1 to 0.12 %, exceptionally 0.17 % at 10.2 m. The TOC content of the Dakhla Formation gradually increases from 0.15 to 0.25 % with the maximum of 0.4 % at 19.2 m, followed by gradual decrease in TOC values from 0.28 to 0.11 %. The uppermost part of the Dakhla Formation, which contains phosphatic beds, shows TOC value 0.14 % at 25.8 m. The chalks of the Tarawan Formation record very low values of 0.11 % TOC at 27.3 m. The obtained TOC values from the base of the Esna Shale Formation are low between 0.14 and 0.21 %, followed by a more or less constant range between 0.12 and 0.1 % in the upper part of the studied section (from 41.1 to 45 m). This observation indicates the oxidization of organic matter in these formations in the outcrops.

At Bir Dakhl, generally the values of TOC are very low. It shows strong TOC depletion in the upper part of Sudr Formation as depicted at 30.9–33.9 m. At the base of Esna Formation, the relative TOC peak 0.1 % (39.9 m) is associated with a minor calcium carbonate depletion (Fig. 2b).

5.2 Benthic foraminifera

5.2.1 Benthic foraminiferal assemblage biofacies

Four main Cretaceous/Palaeogene biofacies of benthic foraminiferal assemblages that characterize bathymetric regimes have been recognized in the studied part of the basin: biofacies A (inner to middle neritic, 50–100 m), biofacies B (outer nertic, 100-200 m), biofacies C (proximal upper bathyal, 200–400 m), and biofacies D (distal upper to middle bathyal, 400–700 m). For detailed benthic foraminiferal assemblage composition see Table 1.

5.2.2 Total foraminiferal number (TFN)

The total foraminiferal number (TFN) in one gram of dry sediment was calculated. In Bir Dakhl (Fig. 2b), TFN

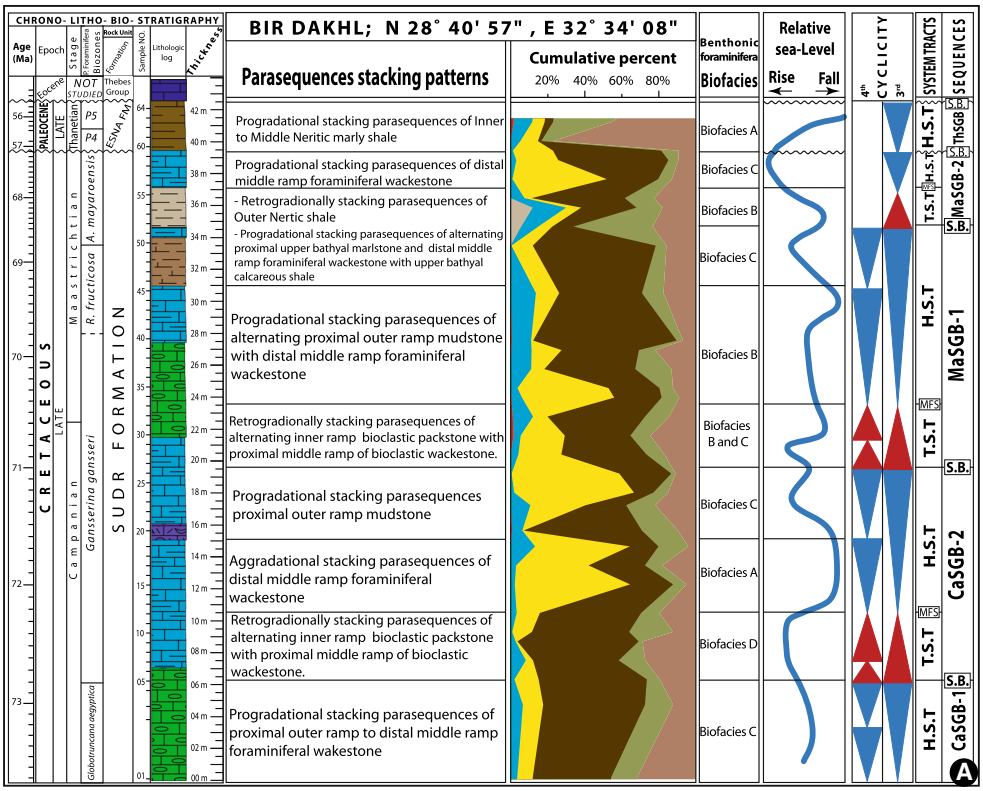
CHRONO- LITHO- BIO- STRATIGRAPHY
BIR DAKHL; N 28° 40' 57" , E 32° 34' 08"
Parasequences stacking patterns
Cumulative percent
20% 40% 60% 80%
Benthonic foraminifera Biofacies
Relative sea-Level
Rise Fall
CYCLICITY
SYSTEM TRACTS
SEQUENCES
Progradational stacking parasequences of Inner to Middle Neritic marly shale
Progradational stacking parasequences of distal middle ramp foraminiferal wackestone
- Retrogradionally stacking parasequences of Outer Nertic shale
- Progradational stacking parasequences of alternating proximal upper bathyal marlstone and distal middle ramp foraminiferal wackestone with upper bathyal calcareous shale
Progradational stacking parasequences of alternating proximal outer ramp mudstone with distal middle ramp foraminiferal wackestone
Retrogradionally stacking parasequences of alternating inner ramp bioclastic packstone with proximal middle ramp of bioclastic wackestone.
Progradational stacking parasequences proximal outer ramp mudstone
Aggradational stacking parasequences of distal middle ramp foraminiferal wackestone
Retrogradionally stacking parasequences of alternating inner ramp bioclastic packstone with proximal middle ramp of bioclastic wackestone.
Progradational stacking parasequences of proximal outer ramp to distal middle ramp foraminiferal wakestone
Biofacies A
Biofacies C
Biofacies B
Biofacies C
Biofacies B
Biofacies B and C
Biofacies C
Biofacies A
Biofacies D
Biofacies C
H.S.T
T.S.T
MFS
S.B.
MaSGB-2
MaSGB-1
CaSGB-2
CaSGB-1
A

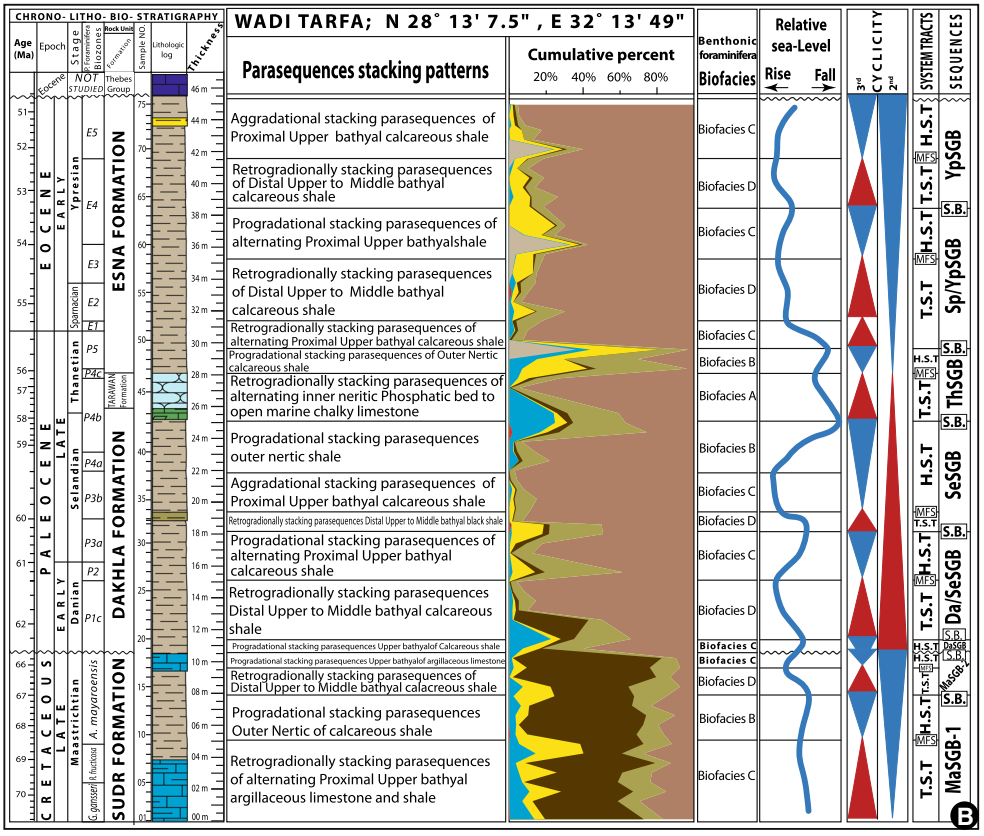
CHRONO- LITHO- BIO- STRATIGRAPHY
WADI TARFA; N 28° 13' 7.5" , E 32° 13' 49"
Parasequences stacking patterns
Cumulative percent
20% 40% 60% 80%
Benthonic foraminifera Biofacies
Relative sea-Level
Rise Fall
CYCLICITY
SYSTEM TRACTS
SEQUENCES
Aggradational stacking parasequences of Proximal Upper bathyal calcareous shale
Retrogradionally stacking parasequences of Distal Upper to Middle bathyal calcareous shale
Progradational stacking parasequences of alternating Proximal Upper bathyalshale
Retrogradionally stacking parasequences of Distal Upper to Middle bathyal calcareous shale
Retrogradionally stacking parasequences of alternating Proximal Upper bathyal calcareous shale
Progradational stacking parasequences of Outer Nertic calcareous shale
Retrogradionally stacking parasequences of alternating inner neritic Phosphatic bed to open marine chalky limestone
Progradational stacking parasequences outer nertic shale
Aggradational stacking parasequences of Proximal Upper bathyal calcareous shale
Retrogradionally stacking parasequences Distal Upper to Middle bathyal black shale
Progradational stacking parasequences of alternating Proximal Upper bathyal calcareous shale
Retrogradionally stacking parasequences Distal Upper to Middle bathyal calcareous shale
Progradational stacking parasequences Upper bathyalof Calcareous shale
Progradational stacking parasequences Upper bathyalof argillaceous limestone
Retrogradionally stacking parasequences of Distal Upper to Middle bathyal calcareous shale
Progradational stacking parasequences Outer Nertic of calcareous shale
Retrogradionally stacking parasequences of alternating Proximal Upper bathyal argillaceous limestone and shale
Biofacies C
Biofacies D
Biofacies C
Biofacies D
Biofacies C
Biofacies B
Biofacies A
Biofacies B
Biofacies C
Biofacies D
Biofacies C
Biofacies C
Biofacies D
Biofacies B
Biofacies C
H.S.T
T.S.T
MFS
S.B.
YpSGB
Sp/YpSGB
ThSGB
SeSGB
Da/SeSGB
MaSGB
MaSGB-1
B

◀**Fig. 3** Estimated palaeo-depth and relative sea-level curves for the Upper Cretaceous–Palaeogene in Bir Dakhl section (**a**) and Wadi Tarfa section (**b**). Summary of chrono-, bio-, and lithostratigraphy, parasequence stacking patterns, cumulative percent of the washed residue components, biofacies, paleobathymetry, and sequence stratigraphic interpretations. *HST* highstand systems tract, *TST* transgressive systems tract, *MFS* maximum flooding surface, *SB* sequence boundary

values display rapid fluctuations in the Late Cretaceous from 4389 to 71 between the Campanian *Globotruncana aegyptiaca* zone and the latest Maastrichtian *Abathomphalus mayaroensis* zone. A significant drop in TFN value is observed in Late Paleocene at the top of *Morozovella velascoensis* zone.

In Wadi Tarfa (Fig. 2a), the TFN shows a regular increase from the Maastrichtian *Gansserina gansseri* zone (TFN of WT-01 = 404) to the Early Paleocene *Praemurica uncinata* zone (TFN of WT-26 = 7655). A remarkable peak of the TFN (up to 16,794) is observed in the Selandian, Late Paleocene (*Igorina albeari* subzone), and a sudden decrease to (178) at the latest Selandian to Thanetian transition (base of *Acarinina subsphaerica* subzone). The Early Eocene displays a gradual increase in TFN, but toward *Morozovella aragonensis/Morozovella*

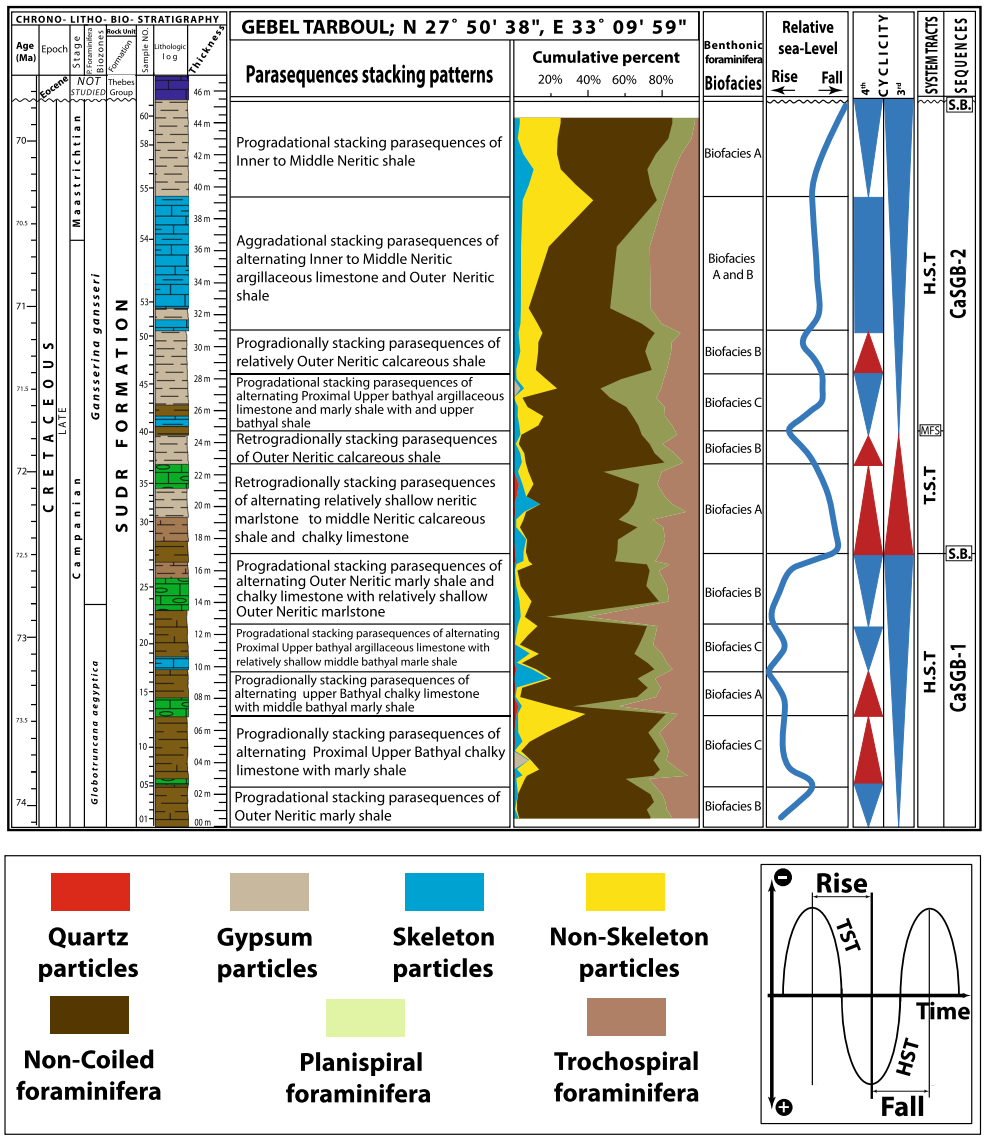

Fig. 4 Estimated palaeo-depth and relative sea-level curves for the Upper Cretaceous Sudr Formation in the Gebel Tarboul section. Summary chrono-, bio-, lithostratigraphy, parasequence stacking patterns, cumulative percent of the washed residue components, biofacies, palaeobathymetry, sequence stratigraphic interpretations. *HST* highstand systems tract, *TST* transgressive systems tract, *MFS* maximum flooding surface, *SB* sequence boundary

Table 1 Detailed benthic foraminiferal assemblages, and bathymetric regimes etablished in the southern Galala Sub-basin

Biofacies	Benthic assemblages	Bathymetric regimes
Biofacies A	*Frondicularia* spp., *Laevidentalina legumen*, *Vaginulinopsis midwayana*, *Gaudryina* sp. and *Spiroplectinella henryi*. Besides the common nominative MF species, of various *Cibicidoides succedens*, *Ramulina navarroana*, *Vaginulina* sp., *Lagena globosa*, *Lagena hispida*, *Bolivina midwayensis*, *Neoflabellina paleocenica*, *Anomalinoides welleri*, *Nodosaria semispinosa*, *Chrysalogonium tappanae*, *Anomalinoides midwayensis*, and *Marginulinopsis tuberculata*	Inner to middle neritic
Biofacies B	Composed of most species of the biofacies A and *Valvulineria* spp., *Tritaxia midwayensis*, *Stilostomella paleocenica*, *Lenticulina cultrate*, and *Neoflabellina semireticulata*	Outer nertic
Biofacies C	*Cibicidoides alleni*, *Chrysalogonium elongatum*, *Dentalina eocenica*, *Cibicidoides vulgaris*, and *Nodosaria semispinosa*	Proximal upper bathyal
Biofacies D	*Gavelinella danica*, *G. dayi*, *Spiroplectinella dentate*, *Cibicidoides alleni*, *Nuttallides truempyi*, *Gavelinella danica* and *Gyroidinoides globosus*	Distal upper to middle bathyal

subbotinae zone, a rapid increase in total foraminiferal number in sample WT-74 (5568) was measured.

5.2.3 Planktonic/benthic ratio (P%)

In the studied sediments, the average P% shows a slight change throughout the Late Cretaceous sediments (Fig. 2). From the *Globotruncana aegyptiaca* zone to the lowermost part of the *Gansserina gansseri* zone, P% values range between 72 and 94 %. In the Middle Campanian and earliest Maastrichtian section, a significant upward increase in P%, ranging between 33 and 58 %, has been recorded. Slight drops of P% are observed in the Late Maastrichtian. The Late Paleocene is also characterize by an abrupt drop in P% (9 % in in sample WT-47). The Early Eocene is characterized by a gradual upward increase in P% from ~80 to 99 % (*Pseudohastigerina wilcoxensis*/*Morozovella velascoensis* zone to *Morozovella aragonensis*/*Morozovella subbotinae* zone).

5.3 Depositional sequences

The study interval that includes the Upper Cretaceous Sudr Formation and the part of the Palaeogene Dakhla, Tarawan, and Esna formations was divided into ten depositional sequences (1–10) that range in approximate duration from 0.5 to 2.5 Myr. Each sequence contains transgressive and highstand systems tracts, whereas the lowstand system tracts are absent in the study area. Sequence thickness increases upwards from sequence 1 to sequence 3 and then decreases from sequence 3 to sequence 6. Such trends implies that accommodation space was increasing, coupled with high subsidence rates and high sediment supply during formation of sequence 1 to sequence 3, and decreasing from the time of sequence 4 toward the transition of Paleocene to Eocene (sequence 10). Each of the studied sequences typically contains a lower retrogradational parasequence set that is bounded above by a maximum-flooding surface and an upper progradational parasequence set that is bounded above by a sequence boundary. Parasequences within parasequence sets are stacked in distinctive transgressive (landward-stepping) and regressive (seaward-stepping) patterns that are indicative of transgressive and highstand systems tracts (TST and HST), respectively. These stacking patterns are commonly expressed as deepening-upward (transgressive) and shallowing-upward (regressive) cycles that are based on foraminifera content, litho-and bio-facies assemblages, and are accompanied by changes in the sediment type and/or TOC content (Figs. 3, 4).

6 Discussion

6.1 Paleoproductivity

The reconstruction of the productivity patterns is of great interest because of the important links to current patterns, mixing of water masses, wind, the global carbon cycle and biogeography. Productivity is often reflected in the flux of carbon into the sediment. Generally, there is a relationship between productivity in surface waters and organic carbon accumulation in the underlying sediments (Sarnthein et al. 1992). Below the central gyres of the ocean and the deserts, the organic carbon content in sediments is extremely low. In upwelling areas, the organic carbon content of the sediments can be extremely high. From this observation, it may be expected that, at any one place, a change in the content of the sediment organic carbon indicates a change in productivity through time (Wefer et al. 1999).

Low carbonate values can indicate the dissolution or dilution of carbonates below the calcite compensation depth (CCD) and/or an increased terrigenous component due to the transportation of weathered exposed rock material to the basin (El Kammar and El Kammar 1996). Carbonate content together with planktonic foraminiferal

numbers and planktonic/benthic ratios can be used to estimate carbonate dissolution (Guasti and Speijer 2007). Enhanced $CaCO_3$ dissolution should increase the benthic/planktic (B/P) foraminiferal ratios. These low contents of $CaCO_3$ have been interpreted as times of increased carbonate dissolution and as a consequence of changes in deep water circulation (Roth et al. 2000).

In Wadi Tarafa, the Dakhla Formation records an increase in carbonate dissolution after ~62 Ma with maximum dissolution of up to 5 % B/P at 60 Ma. In contrast to the deep sea, shelf deposits are largely unaffected by dissolution due to lysocline shallowing during Early Palaeogene hyperthermals (John et al. 2008). This is clearly visible in the lowermost part of the Sudr Formation, which consists mainly of hemipelagic argillaceous limestone, and therefore shows maximum carbonate content.

On the other hand, strongly varying sedimentation rates and bulk rock calcium carbonate fluctuations are interpreted as a result of multiple unconformities and not of dissolution or dilution of carbonates (Zachos et al. 2006; Giusberti et al. 2007; Galeotti et al. 2010). The local environmental and tectonic constraints of the Galala succession reveal a combination of siliciclastic dilution and tectonic unconformities as major triggers for calcium carbonate depletion (Höntzsch et al. 2011). In Wadi Tarafa, high fluctuations of calcium carbonate content in the Early Eocene (Fig. 2a) are related to intensive siliciclastic dilution during Wadi Araba uplift and the re-deposition of Mesozoic and Palaeozoic sandstones (Kuss et al. 2000; Scheibner et al. 2001; Höntzsch et al. 2011). The well visible depleted calcium carbonate ratios in *Pseudohastigerina wilcoxensis/Morozovella velascoensis* concurrent-range zone (E2) are seen when the tectonic activity of the Syrian Arc decreases significantly (Moustafa and Khalil 1995; Hussein and Abd-Allah 2001; Höntzsch et al. 2011).

Hyperthermal events contribute significantly to the global carbon circulation and carbonate depletion. At the Paleocene Eocene Thermal Maximum (PETM) level in Wadi Tarafa, calcium carbonate depletion reaches to more than 65 %.

Therefore, we conclude that dissolution is not the only controlling factor on the $CaCO_3$ minima in the studied sections that correspond in time to the global "Carbonate Crash". The tectonic processes and hyperthermal events (e.g. PETM) could contribute to the depletion of the carbonate contents.

Geological evidence indicates that organic-rich sediments could be deposited even on open shelf until the early Palaeozoic period, but they could be deposited only in a hydrologically isolated basins afterwards (Klemme and Ulmishek 1991). According to our result, the sediments of Wadi Tarafa are characterized by generally low total organic carbon values, which can be related to higher sedimentation rates and to siliciclastic dilution on the platform (Fig. 2). TOC-rich horizons in the Dakhla Formation of Early Palaeogene are interpreted as black shales which were driven by local upwelling regimes (Speijer and Wagner 2002). A single black shale which is significantly enriched in TOC correlates with calcium carbonate depletion of the post-PETM hyperthermal event (TOC_{PETM} ~ 0.40 %) and probably reflects transient productivity (Hallock et al. 1991; Scheibner et al. 2005; Sluijs et al. 2009). The Early Eocene Esna shales reveal very low TOC values which suggest an open ocean environment with low terrigenous influx from the African craton (Speijer and Wagner 2002).

6.2 Paleobathymetry

A common goal in basin analysis is the assessment of palaeobathymetry for interpreting depositional environments, constructing the subsidence and uplift history, and other aspects of basin evolution. Various studies indicated that the comparative abundance of planktic and benthic foraminiferal assemblages could record sea-level fluctuations curve, and could be useful for interpreting the paleobathymetry of sediments (Buzas and Gibson 1969; Olsson and Wise 1987; Olsson 1991). The geometry of this curve (hinge and inflection points, positive/negative/constant trends) is used to estimate the approximate position of candidates for systems tract boundaries. The value of the P% ratio strongly increases in deeper waters and eventually approach infinity (P/B ratio increase in the depth range of 0–1000 m from 0 to 10, and then rapid increase from 20 to ∞). In this study, the following bathymetric divisions were applied in agreement with Van Morkhoven et al. (1986) and Berggren and Miller (1989): neritic <200 m; upper bathyal 200–600 m; middle bathyal 600–1000 m; lower bathyal 1000–2000 m; upper abyssal 2000–3000 m; lower abyssal >3000 m). Based on water depth zonation of Van Morkhoven et al. (1986), the depositional depth of the studied sections varies from ~50 to ~750 m, indicating an environment range from the middle neritic to the bathyal zone (Fig. 2). The most widely applied method for assessing paleobathymetry is the analysis of benthic foraminiferal biofacies. In the present study, the overall nature of the benthic foraminiferal assemblages is examined to prove the validity of palaeo-depth estimations obtained using the percentage of planktic foraminifera. We combine benthic foraminiferal biofacies, palaeo-productivity (TOC and carbonate content) and two-dimensional palaeo-water depth to construct a two-dimensional palaeo-slope or palaeo-bathymetric models. Palaeo-slope modeling is based on the assumption that benthic foraminiferal biofacies horizontally occupy distinct environments but integrate and replace each other vertically with a depositional

environment change. Additionally, any significant trends in palaeobathymetry can be checked along the succession by identifying marker species for selected depth intervals. Based on this information, the bathymetric evolution of the investigated sections can be reconstructed. The benthic assemblages in the studied sediments indicate an upper to deep middle bathyal environment, and being dominated by biofacies A, B and C assemblages. The benthic assemblages of samples WT-70 to WT-75, however, are dominated by a biofacies B associated with the normally shallow-water preferences of *Laevidentalina species*, *Anomalinoides* species and absence of deep benthic foraminiferal assemblage. This suggests that these samples were deposited at upper bathyal palaeo-depths (Figs. 3, 4).

Olsson and Nyong (1984) have shown that the inner shelf (10–50 m) is characterized by rare planktonics (<8 %) with low species diversity, while relatively P% of 8–25 % characterizes the middle shelf (50–100 m) with increased species diversity. On the other hand, the outer shelf environment (100-200 m) is characterized by high P% of 70 %, while P% of 90 % is attributed to the middle slope (400–800). According to Mendes et al. (2004), the benthic foraminiferal number (BFN) is inversely related with water depth. Slightly increased BFN in the lowermost part of the Gebel Tarboul section (BFN of EM-06 is 693) indicates that at this stratigraphic level bottom water conditions have been generally more favorable for the production of benthic foraminifera.

6.3 Depositional environments and sequence stratigraphy

The interpretation of depositional environment geometries and depositional cycles allowed the recognition of ten (3rd-order) depositional sequences in Cretaceous–Palaeogene strata that are bounded by 10 sequence boundaries. The sequence stratigraphic interpretations are shown in Table 2, Figs. 3 and 4. Finally the idealized Late Cretaceous–Early Palaeogene sea-level fluctuations in the Southern Galala Sub-basin, as derived from integrated lithostratigraphy, micropaleontology, paleobathymetry, organic geochemistry are depicted in Fig. 5. The recognized ten (third order) depositional sequences in Cretaceous–Palaeogene are as follow:

6.3.1 SEQ-1: CaSGB-1 sequence

CaSGB-1 sequence represents the first studied depositional cycle in South Galala Sub-basin. This sedimentary cycle that covers a time interval of approximately 1.7 Myr within the latest Campanian, stratigraphically comprises the lowermost part of Markha Member of Sudr Formation. This cycle involves the differentiation of HST deposits only because the TST deposits are not exposed. Moreover, the CaSGB-1 sequence represents the basal part of Gebel Tarboul and Bir Dakhl section and is not present in Wadi Tarfa. Following the sequence hierarchy definition of Vail et al. (1991), this sedimentary cycle is of third-order cycle rank, consisting of many fourth-order subcycles (Table 2). Deepening-upward subcycles are composed of a succession dominated by background sedimentation marls with thin intercalated chalky limestone beds. Shallowing-upward subcycles are dominated by foraminiferal wackestone to marly shale with relatively high planktonic foraminiferal percentages. They are interpreted to represent aggradational to progradational stacking patterns.

6.3.2 SEQ-2: CaSGB-2 sequence

The CaSGB-2 sequence spans the Markha Member and Abu Zeneima Member of the Sudr Formation at Gebel Tarboul (Fig. 4), and the Markha Member at Bir Dakhl. It can be treated as siliciclastic/carbonate mixed system (shallow-water, hemipelagic, and pelagic) deposited during ~2.9 Myr. Basin-wide and local tectonism during Cretaceous resulted in subsidence along the fault system situated in shoulders of the Southern Galala Sub-basin, with higher subsidence rates in Gebel Tarboul than Bir Dakhl during CaSGB-2 deposition. This difference has resulted in increased thickness of deep-marine pelagic shales with higher planktonic foraminiferal abundance intercalated with thin beds of hemipelagic carbonate at Gebel Tarboul. This contrasts to dominating hemipelagic carbonates in Bir Dakhl.

6.3.3 SEQ-3: MaSGB-1 sequence

Stratigraphically, the MaSGB-1 sequence (~18 m thick.) represents the interval between Markha Member and Abu Zeneima Member of the Sudr Formation and covers a time interval of approximately 3.2 Myr from the latest Campanian to the Late Maastrichtian at Bir Dakhl. At Wadi Tarfa it corresponds to a part of the Abu Zeneima Member (~8 m thick). Typically, it consists of alternations of thick to medium beds of limestones, green marls, and calcareous shale.

6.3.4 SEQ-4: MaSGB-2 sequence

MaSGB-2 sequence covers the time interval of latest Maastrichtian. It is ~2.7 m thick in the uppermost part of Sudr Formation in Wadi Tarfa and ~2.4 m in Bir Dakhl section. This sequence and overlying sequences fade out in the Gebel Tarboul section, which may be interpreted to reflect local deep erosion during the MaSGB-2 sea level fall, associated with local tectonic uplift and basin

Table 2 Summary of depositional sequences and subsequences in Cretaceous–Palaeogene interval of the southern Galala Sub-Basin

Sequences	Subsequences	Time interval	System tracts	Stratigraphy	Occurrence
SEQ-1: CaSGB-1	Post-CaSGB-1 HST	1.7 Myr within the latest Campanian	HST	Lowermost part of Markha Member of Sudr Formation	Basal part of Gebel Tarboul and Bir Dakhl sections
SEQ-2: CaSGB-2	Post-CaSGB-2 TST;CaSGB-2, Post-CaSGB-2 HST	~2.9 Myr Campanian	HST, TST	Markha Member and Abu Zeneima Member of Sudr Formation	Gebel Tarboul and Bir Dakhl sections
SEQ-3: MaSGB-1	Post-MaSGB-1 TST; MaSGB-1. Post-MaSGB-1 HST	3.2 Myr from latest Campanian to Late Maastrichtian	TST, HST	Markha Member and Abu Zeneima Member of Sudr Formation	Bir Dakhl and Wadi Tarfa
SEQ-4: MaSGB-2	Post-MaSGB-2 TST; MaSGB-2, Post-MaSGB-2 HST	latest Maastrichtian	TST, HST	Uppermost part of Sudr Formation	Bir Dakhl and Wadi Tarfa
SEQ-5: DaSGB	Post-DaSGB HST	Late Early Paleocene	TST, HST	Lowermost part of the Dakhla Formation	Wadi Tarfa
SEQ-6: Da/SeSGB	Post-Da/SeSGB TST; Da/SeSGB; Post-Da/SeSGB HST	Latest Danian–Selandian	TST and HST	Dakhla Formation	Wadi Tarfa
SEQ-7: SeSGB	Post-SeSGB TST; SeSGB; Post-SeSGB HST	2.2 Myr Selandian	TST, HST	Dakhla Formation	Wadi Tarfa
SEQ-8: ThSGB	Post-ThSGB TST; ThSGB; Post-ThSGB HST	2.5 Myr Thanetian	TST, HST	Uppermost part of Dakhla Formation, Tarawan Formation	Wadi Tarfa and Bir Dakhl
SEQ-9: Sp/YpSGB	Post-Sp/YpSGB TST; Sp/YpSGB; Post-Sp/YpSGB HST	1.4 Myr Sparnacian	TST, HST	Lower part of Esna Formation	Wadi Tarfa
SEQ-10: YpSGB	Post-YpSGB TST; YpSGB; Post-YpSGB HST	At least 2.5 Myr in Middle to Late Ypresian	TST, HST	Esna Formation	Wadi Tarfa

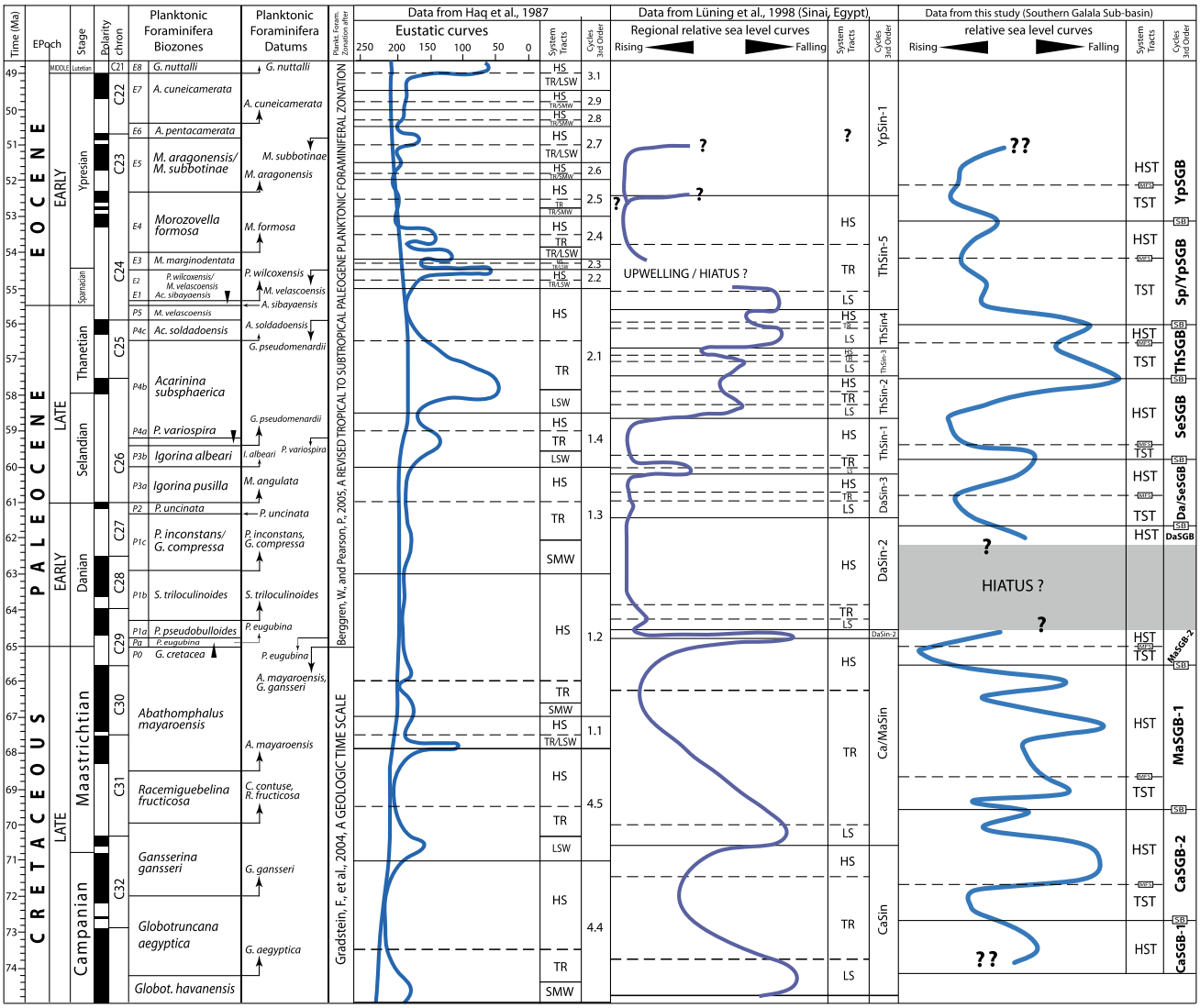

Fig. 5 Idealized Late Cretaceous–Palaeogene sea-level fluctuation curve in southern Galala Sub-Basin, as deduced from integrated lithostratigraphy, micropaleontology, paleobathymetrical parameters, organic geochemistry, and microfacies analysis, and compared with regional and global sea-level variations (Haq et al. 1987; Lüning et al. 1998)

irregularity. This uplift continued until the beginning of the Late Paleocene.

6.3.5 SEQ-5: DaSGB sequence

The DaSGB sequence represents ~1 m of the lowermost part of the Dakhla Formation. It consists of one progradational parasequence forming a shallowing upward cycle of calcareous shale and is attributed to the late Early Paleocene. The basal part of DaSGB sequence is Sequence Boundary type-1 (sequence boundary MaSGB-2). The regional unconformity between chalky limestone (Sudr Formation, Cretaceous) and overlying hard calcareous shale (Dakhla Formation, Paleocene) is characterized by a significant biostratigraphic hiatus demonstrated by the absence of four planktonic foraminifera biozones. The low thickness of this sequence may be result of the magnitude of the K/Pg hiatus that involved removal of LST and TST deposits of this sequence or a non-depositional phase.

6.3.6 SEQ-6: Da/SeSGB sequence

During the Late Danian, an extensive marine transgression took place, leading to the landward shift of the shoreline as far south as northern Sudan (Lüger 1985). In the South Galala Sub-basin, the Late Danian relative sea-level rise started with the formation of landward-stepping middle bathyal shale strata (Da/SeSGB, P1c Sub-zone; Fig. 3). This sea level rise was followed by progradational, proximal upper bathyal shale during the latest Danian-Selandian

(P2 Zone and P3a Sub-zone) due to a slow and localized relative sea-level fall. The Da/SeSGB sequence (~5.5 m thick.) itself can be subdivided into two system tracts (TST and HST), each containing distinct benthic foraminiferal assemblages.

6.3.7 SEQ-7: SeSGB sequence

The ~7 m thick Selandian SeSGB sequence is bounded at its top by a third-order sequence boundary (type-2). It has duration of approximately 2.2 Myr with a sedimentation rate of ~5.5 mm kyear^{-1}.

6.3.8 SEQ-8: ThSGB sequence

The ThSGB sequence in the southern Galala Sub-Basin is represented throughout the interval between Dakhla, Tarawan, and Esna formations and represents a mixed siliciclastic-carbonate succession. It is attributed to Late Paleocene with an estimated duration of ~2.5 Myr.

6.3.9 SEQ-9: Sp/YpSGB (type-2 sequence) sequence

Sp/YpSGB sequence is approximately ~8.5 m thick, deposited throughout the interval between the Late Paleocene (latest Thanetian) and Early Eocene (early Ypresian) and has an approximate duration of 1.4 Myr (third order sequences). It correlates with the lower part of Esna Formation.

6.3.10 SEQ-10: YpSGB sequence

YpSGB sequence comprises the uppermost studied depositional cycles in southern Galala Sub-Basin. It is developed within the upper part of the Esna Formation in Wadi Tarfa and fades out toward the north and south shoulders of the basin. It includes the planktonic foraminiferal Zone E4 and E5 and is assigned to the Early Eocene (middle to late Ypresian). A tentative and minimal estimate for the duration of YpSGB sequence is at least 2.5 Myr with a sedimentation rate of ~2.8 mm kyear^{-1}. The YpSGB sequence is divided into two systems tracts (TST and HST) by a bivalve (*Oyster*) shell bed at 41.5 m.

7 Conclusions

The result of our high resolution analysis of the Late Cretaceous–Early Palaeogene succession in the study area can be summarized as follow: Based on morphology, life position, feeding habitat and environment, four benthic foraminiferal assemblages (biofacies A–biofacies D) have been distinguished. Four carbonate crash events (abrupt drops in carbonate content) during the Cretaceous–Palaeogene interval have been recognized. The depositional environments can be interpreted to range from neritic to middle bathyal (~700 m) depth. Ten third order depositional sequences, each bounded by a sequence boundary, have been described, and only the transgressive and highstand system tracts are preserved. These sequences are controlled by both eustatic sea-level changes and tectonic activities that prevailed during the deposition.

Acknowledgments This project was supported by King Saud University, Deanship of Scientific Research, and College of Science Research Center. The Department of Geology, South Valley University, Egypt, is thanked for the logistic support during the field trip. We wish to thank Prof. Dr Michal Kucera, Bremen University for his comments and valuable discussions. The authors gratefully acknowledged the General Petroleum Company for the hospitality during the field trip. Finally, we would like to express our gratitude to Dr. Sherif Farouk, Egyptian Petroleum Research Institute (EPRI), Cairo, for various kinds of helpful assistance and comments.

References

Aal, A., & Lelek, J. (1994). Structural development of the Northern Sinai, Egypt and its implications on the hydrocarbon prospectivity of the Mesozoic. *Geo Arabia, 1*, 15–30.

Abdel-Kireem, M. R., & Abdou, H. F. (1979). Upper Cretaceous-Lower Palaeogene planktonic foraminifera from South Galala Plateau, Eastern Desert, Egypt. *Revista Española de Micropaleontologia, 11*(2), 175–222.

Awad, G. H., & Abdallah, A. M. (1966). Upper Cretaceous in Southern Galala, Eastern Desert with emphasis on Neighbouring areas. *Journal Geological Soceity of Egypt, 10*, 125–144.

Bandel, K., & Kuss, J. (1987). Depositional environment of the prerift sediments: Galala Heights (Gulf of Suez, Egypt). *Berliner geowissenschaftliche Abhandlungen, 78*, 1–48.

Bandel, K., Kuss, J., & Malchus, N. (1987). The Sediments of Wadi Qena area, Eastern Desert, Egypt. *Journal of African Earth Sciences, 6*, 427–455.

Bengtsson, L., & Enell, M. (1986). Chemical analysis. In B. E. Berglund (Ed.), *Handbook of holocene palaeoecology and palaeohydrology* (pp. 423–454). Chichester: Wiley.

Berggren, W. A., & Miller, K. G. (1989). Cenozoic bathyal and abyssal calcareous benthic foraminiferal zonation. *Micropaleontology, 35*, 308–320.

Berggren, W. A., Kent, D. V., Swisher, C. C. III., & Aubry. M. P. (1995). A revised Cenozoic geochronology and chronostratigraphy. In W. A. Berggren, D. V. Kent, C. C. III. Swisher, M. P. Aubry, J. Hardenbol (Eds.), *Geochronology, time scales and global stratigraphic correlation*, vol. 54 (pp. 129–212). Tulsa: Society for Sedimentary Geology, Special Publications.

Buzas, M. A., & Gibson, T. G. (1969). Species diversity: Benthonic foraminifera in western North Atlantic. *Science*, *163*, 72–75.

El Kammar, A. M., & El Kammar, M. M. (1996). Potentiality of chemical weathering under arid conditions of black shales from Egypt. *Journal of Arid Environments, Z3*, 179–199.

Galeotti, S., Krishnan, S., Pagani, M., Lanci, L., Gaudio, A., Zachos, J. C., et al. (2010). Orbital chronology of Early Eocene hyperthermals from the Contessa Road section, central Italy. *Earth and Planetary Science Letters, 290*, 192–200.

Garfunkel, Z., & Bartov, Y. (1977). The tectonics of the Suez Rift. *Bulletin of Geological Survey of Israel, 71*, 1–44.

Giusberti, L., Rio, D., Agnini, C., Backman, J., Fornaciari, E., Tateo, F., & Oddone, M. (2007). Mode and tempo of the Paleocene–Eocene thermal maximum in an expanded section from the Venetian pre-Alps. *Geological Society of America Bulletin, 119*, 391–412.

Guasti, E., & Speijer, R. P. (2007). The Paleocene–Eocene thermal maximum in Egypt and Jordan: An overview of the planktic foraminiferal record. In S. Monechi, R. Coccioni, & M. R. Rampino, (Eds.), Large ecosystem perturbations: Causes and consequences (pp. 53–67). Geological Society of America, Special Paper 424.

Hallock, P., Premoli-Silva, I., & Boersma, A. (1991). Similarities between planktonic and larger foraminiferal evolutionary trends through Palaeogene paleoceanographic changes. *Palaeogeography, Palaeoclimatology, Palaeoecology, 83*, 49–64.

Haq, B. U., Hardenbol, J., & Vail, P. R. (1987). The chronology of fluctuating sea-level since the Triassic. *Science, 235*, 1156–1167.

Hefny, M., & Youssef, M. (2015). Biostratigraphy and stage boundaries of the upper Cretaceous–early Palaeogene successions in southern Galala area, North-Eastern Desert, Egypt. *Historical Biology, 27*, 68–89.

Hendriks, F., Lüger, P., Bowitz, J., & Kallenbach, H. (1987). Evolution of the depositional enviroments of SE Egypt during the Cretaceous and Lower Palaeogene. *Berliner geowissenschaftliche Abhandlungen, 75*, 49–82.

Höntzsch, S., Scheibner, C., Guasti, E., Kuss, J., Marzouk, A., & Rasser, M. (2011). Increasing restriction of the Egyptian shelf during the Early Eocene?—New insights from a southern Tethyan carbonate platform. *Palaeogeography, Palaeoclimatology, Palaeoecology, 302*, 349–366.

Hussein, I. M., & Abd-Allah, A. M. A. (2001). Tectonic evolution of the northeastern part of the African continental margin, Egypt. *Journal of African Earth Sciences, 33*, 49–68.

Ismail, A. A. (2012). Late Cretaceous–Early Eocene benthic foraminifera from Esh El Mallaha area, Egypt. *Revue de Paléobiologie, Genéve, 31*, 15–50.

Ismail, A. A., Hussein-Kamel, Y. F., Boukhary, M., & Ghandour, A. A. (2009). Late Cenomanian-Early Turonian foraminifera from Eastern Desert, Egypt. *Micropaleontology, 55*, 396–412.

John, C. M., Bohaty, S. M., Zachos, J. C., Sluijs, A., Gibbs, S., Brinkhuis, H., & Bralower, T. J. (2008). North American continental margin records of the Paleocene–Eocene thermal maximum: Implications for global carbon and hydrological cycling. *Paleoceanography, 23*, 1–20.

Klemme, H. D., & Ulmishek, G. F. (1991). Effective petroleum source rocks of the world: Stratigraphic distribution and controlling depositional factors. *Bulletin-American Association of Petroleum Geologists, 75*, 1809–1851.

Krenkel, E. (1925). *Geologie Afrikas*. Berlin: Bornträger.

Kuss, J. (1992). The Aptian-Paleocene shelf carbonates of northeastern Egypt and southern Jordan: establishment and break-up of carbonate platfoms along the southern Tethyan shores. *Zeitschrift der deutschen geologischen Gesellschaft, 143*, 107–132.

Kuss, J., & Leppig, U. (1989). The early Palaeogene (middle-late Paleocene) limestones from the western Gulf of Suez, Egypt. *Neues Jahrbuch Geologie Pallontologie Abhandlungen, 177*, 289–332.

Kuss, J., Westerhold, T., Groá, U., Bauer, J., & Lüning, S. (2000). Mapping of Late Cretaceous stratigraphic sequences along a Syrian Arc Uplift—Examples from the Areif el Naqa/Eastern Sinai. *Middle East Research Center, Ain Shams University, Earth Science Services, 14*, 171–191.

Lüning, S., Marzouk, A. M., & Kuss, J. (1998). The Palaeocene of Central East Sinai, Egypt: Sequence stratigraphy' in monotonous hemipelagites. *The Journal of Foraminiferal Research, 28*(1), 19–39.

Mendes, I., Gonzalez, R., Dias, J. M. A., Lobo, F., & Martins, V., (2004). Factors influencing recent benthic foraminifera distribution on the Guadiana shelf (Southwestern Iberia). *Marine Micropaleontology*, *51*, 171–192.

Moustafa, A. R., & Khalil, M. H. (1995). Superposed deformation in the northern Suez Rift, Egypt: Relevance to hydrocarbons exploration. *Journal of Petroleum Geology, 18*, 245–266.

Olsson, R. K. (1991). Cretaceous to Eocene sea-level fluctuations on the New Jersey margin. *Sedimentary Geology, 70*, 195–208.

Olsson, R. K., & Nyong, E. E. (1984). A paleoslope model for Campanian-Lower Maastrichtian Foraminifera of New Jersey and Delaware. *Journal of Foraminiferal Research*, *14*, 50–68.

Olsson, R. K., & Wise, S. W., Jr. (1987). Upper Maastrichtian to middle Eocene stratigraphy of the New Jersey slope and coastal plain. In J. E. van Hinte, Wise, S. W., Jr., et al., Initial report DSDP, 93, (pp. 1343–1365)

Philip, J., & Floquet, M. (2000). Late Cenomanian (94.7-93.5). In J. Dercourt, M., Gaetani, B., Vrielynck, E., Barrier, B., Biju-Duval, M. F., Brunet, J. P., Cadet, S., Crasquin, M., & Sandulescu (Eds.), Atlas peri-tethys palaeogeographical maps. CCGM/CGMW (pp. 129–136).

Picard, L. (1943). Structure and Evolution of Palestine, with comparative notes on neighboring countries. *Bulletin Geology Department Hebrew University*, *4*, l–34.

Rosenthal, E., Weinberger, G., Almogi-Labin, A., & Flexer, A. (2000). Late Cretaceous-early Palaeogene development of depositional basins in Samaria as a reflection of eastern Mediterranean tectonic evolution. *Bulletin-American Association of Petroleum Geologists, 84*, 997–1114.

Roth, M. J., Droxler, A. W., & Kameo, K. (2000). The Caribbean carbonate crash at the Middle to Late Miocene transition: Linkage to the establishment of the modern global ocean conveyor. In R. M. Leckie, H., Sigurdsson, G. D., Acton, & G., Draper, (Eds.), Proceedings of ODP, Scientific Research, vol. 165 (pp. 249–273): College Station: Ocean Drilling Program.

Said, R. (1962). *The geology of Egypt*. Amsterdam, New York: Elsevier. **397 pp**.

Sarnthein, M., Pflaumann, U., Ross. R., Tiedemann, R., & Winn, K. (1992). Transfer functions to reconstruct ocean productivity: a comparison. In C. P. Summerhayes. W. L., Prell, & K. C. Emeis (Eds.), Upwelling systems: Evolution since the early Miocene. Geological Society London, vol. 64, (pp. 411–427), Special Publications.

Scheibner, C., Kuss, J., & Marzouk, A. (2000). Slope sediments of a Paleocene ramp-to-basin transition in NE Egypt. *International Journal of Earth Science, 88*, 708–724.

Scheibner, C., Marzouk, A. M., & Kuss, J. (2001). Shelf architectures of an isolated Late Cretaceous carbonate platform margin, Galala Mountains (Eastern Desert, Egypt). *Sedimentary Geology, 145*, 23–43.

Scheibner, C., & Speijer, R. P. (2009). Recalibration of the Tethyan shallow-benthic zonation across the Paleocene–Eocene boundary: The Egyptian record. *Geologica Acta, 7*, 195–214.

Scheibner, C., Speijer, R. P., & Marzouk, A. M. (2005). Larger foraminiferal turnover during the Paleocene/Eocene thermal maximum and paleoclimatic control on the evolution of platform ecosystems. *Geology, 33*, 493–496.

Sluijs, A., Schouten, S., Donders, T. H., Schoon, P. L., Rohl, U., Reichart, G. J., et al. (2009). Warm and wet conditions in the Arctic region during Eocene thermal maximum 2. *Nature Geoscience, 2*, 777–780.

Speijer, R. P., & Wagner, R. (2002). Sea-level changes and black shales associated with the late Paleocene thermal maximum; organic-geochemical and micropaleontologic evidence from the

southern Tethyan margin (Egypt-Israel). In C. Koeberl & K. G. MacLeod (Eds.), *Catastrophic events and mass extinctions: Impacts and beyond* (pp. 533–549). Boulder: Geological Society of America Special Paper.

Vail, P. R., Audemard, F., Bowman, S. A., Eisner, P. N., & Perez Cruz, C. (1991). The stratigraphic signatures of tectonics, eustasy and sedimentology—an overview. In G. Einsele, W. Ricken, & A. Seilacher (Eds.), *Cycles and events in stratigraphy* (pp. 617–659). Berlin: Springer.

Van Morkhoven, F. P., Berggren, W. A., & Edwards, A. S. (1986). Cenozoic cosmopolitan deep-water Benthic Foraminifera. *Bulletin du Centre des Recherches Explorattoire et Productive, Elf-Aquitaine, Memoires, 11*, 1–421.

Wefer, G., Berger, W. H., Bijma, J., & Fischer, G. (1999). Clues to ocean history: A brief overview of proxies. In G. Fischer, & G. Wefer (Eds.), Use of proxies in paleoceanography: Examples from the South Atlantic (pp. 1–68), Berlin: Springer.

Zachos, J. C., Schouten, S., Bohaty, S., Quattlebaum, T., Sluijs, A., Brinkhuis, H., et al. (2006). Extreme warming of mid-latitude coastal ocean during the Paleocene–Eocene thermal maximum: Inferences from TEX86 and isotope data. *Geology, 34*, 737–740.